A study on the effect of process parameters on feature resolution in 3D inkjet printing

Karin J. Chen[1] , Ahmed Elkaseer[1,2], Steffen G. Scholz[1,2]

[1] Karlsruhe Institute of Technology, Hermann-von-Helmholtz-Platz 1, 76344 Eggenstein-Leopoldshafen, Germany
2 Karlsruhe Nano Micro Facility (KNMFi), Karlsruhe Institute of Technology, Karlsruhe, Germany
karin.chen@kit.edu

Abstract

Among the existing additive manufacturing (AM) technologies, 3D inkjet printing (3D-IJP), also known as material jetting, enables fabrication of intricate multi-materials parts with resolution and accuracy in the order of few microns. In 3D-IJP, a piezo-based printhead generates tiny droplets on a substrate which merge upon impact. The printing is followed by a curing step to solidify the wet printed layer before continuing with the next layer. The resulting print quality is governed by numerous process parameters. The aim of this investigation is to determine the influence of the process parameters UV-exposure time and print-velocity on the achievable feature resolution of the 3D printed part based on the USAF MIL-STD-150A resolution test chart. The trials were conducted on a 3D inkjet printer and a transparent UV-curable ink was used. This study showed that the USAF test coupon serves well to study the effect of printing parameters on feature resolution qualitatively. Several heights (0.5 mm to 2 mm) of the USAF test chart group 0 have been printed. Each group is made of three vertical and three horizontal lines. The printed lines were assessed based on a three-level grading system (partial merge = 2 of 3 adjacent lines merged, full merge = 3 of 3 lines merged, or no merging). The specimens were printed on a base layer printed with the same material in order to decouple the obtained results from the substrate properties. The applied aspect ratios (1 to 7.13) did not have any influence on the merging behavior, while a longer UV-exposure was able to resolve smaller features. The improvement of feature resolution by lowering the print-velocity was not as significant as when increasing the UV-exposure time and could only be observed for the lines perpendicular to print direction. The smallest resolvable element printed in this investigation was 353.55 µm for lines in print direction which were subject to a curing of 100 ms exposure time at 4 W/cm^2 UV-irradiance. The closest distance that could be resolved for the lines perpendicular to the print direction without any merging was 396.85 µm.

Keywords: 3D inkjet printing, additive manufacturing, 3D printing, UV-curable ink, feature resolution, UV-dosage, print speed, print frequency,

1. Introduction

The ability of additive manufacturing (AM) to create products of complex geometries and properties revolutionized many industries in their thinking and approach to their own products. AM has not only proven useful during the COVID-19 pandemic for producing protective gadgets and healthcare utensils [1-3], but is currently implemented for building houses and bridges [4, 5] as well. AM is a generic term which describes manufacturing technologies that fabricate 3D parts in a layer-wise manner [6]. Among these additive manufacturing technologies, 3D inkjet printing (3D-IJP), also known as material jetting, offers particular potentials to fabricate intricate multi-materials parts with resolution and accuracy in the order of few microns. In 3D-IJP, a piezo-based printhead generates tiny droplets on a substrate (or the previous printed layer) which merge upon impact. The printing is followed by a curing step to solidify the wet printed layer before continuing with the next layer. The resulting print quality is governed by numerous process parameters. Waveform [7], droplet volume [8], substrate-to-printhead distance and print/chuck-velocity [9], for example, determine the droplet shape ejected from the printhead and the deposition accuracy of the droplet on the substrate. Print resolution [10] or curing parameters such as UV-dosage [11], curing strategy [12] and time between droplet impact and curing [13] influence the shape of the solidified printed layer on the substrate and eventually the geometrical dimensions of the printed pattern. Well-chosen curing settings could avoid saggy edges [12], or warping or increased brittleness due to over-curing [14]. UV-dosage can be either adjusted by the curing duration or the UV-radiation intensity [15]. The aim of this study is to investigate how UV-exposure time and print-velocity influence the feature resolution limit of a 3D printed structure.

2. Materials and Methods

The 3D inkjet printer used for this experiment is named “njet 3D”, provided by Notion Systems.

Fig. 1. 3D inkjet printer “njet 3D” by Notion Systems

The printer is equipped with the printhead KM1024iLHE30 which is able to eject 1024 droplets at the same time with a nominal droplet volume of 30 pl.

The printhead's native resolution is 360 dpi. The specimens were printed with a UV-curable ink provided by the machine supplier Notion Systems. The ink is cured by the UV-LED device Phoseon FireEdge FE400 with rod optics, 80 mm x 10 mm emission window and emitting radiation at 365 nm wavelength. The rod optics ensure that the exposed area remains the same for all distances between the substrate and the UV-LED which means that the UV-intensity (power/area) stays constant.

The 1951 United States Air Force (USAF) resolution test chart was selected for evaluating the achievable feature resolution (see Fig. 2). This test chart contains horizontal and vertical lines which are spaced with the same distance apart as the width of the neighbouring lines. In this study, the test pattern is aligned in a way, that the vertical lines are parallel to the print direction (PD), while the horizontal lines are aligned perpendicular to the print direction (PD90°). Each group contains 6 elements, with element 1 being the one with the greatest spatial periodicity. One period consists of one black line and one white area.

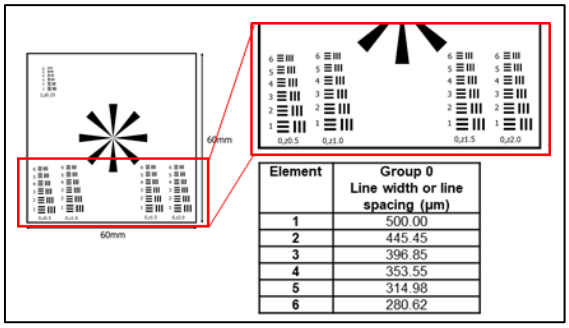

Fig. 2. Print image (binary TIFF-file) based on the USAF MIL-STD-150A resolution test chart. The structure of interest of this investigation is group number 0 (red frame)

The resolution limit can be determined by looking at the printed element that cannot be distinguished any more due to merging. For this investigation, only the test chart group number 0 has been considered since the lines of group 1 all merged, while group -1 were all well-separated. The Siemens star should offer some insights into the dimensional and edge accuracy in print and perpendicular to print direction, however it was not further examined for this study. Fig. 2 shows the print file (TIFF-format) which served as the input file for the printer. The line width and spacing of the four structure on the lower half of the image corresponds to the dimensions defined in the standard of USAF MIL-STD-150A. Each column represents one particular height (from left to right: 0.5 mm, 1.0 mm, 1.5 mm, 2.0 mm). The corresponding line width/line spacing values of each element are shown in Fig. 2 as well. The total dimension of the printed specimens is 60 mm x 60 mm. This width was chosen in order to not exceed the width of the printhead, which is for this particular printhead 72 mm, and to address as many nozzles as possible to consider the spatial reproducibility of the printed specimens.

Each print condition was applied triple times. Print-velocity (400 mm/s and 200 mm/s) and UV-exposure time (50 ms and 100 ms) were the only parameters modified within this experiment, resulting in a total number of 12 specimens. The UV-exposure time is adjusted by varying the UV-velocity (200 mm/s and 100 mm/s). The degree of curing is governed by the amount of UV-dose D_{UV} (J/m^2) which is defined as the temporal integral of UV-intensity I_{UV} (W/m^2) [15] (see Eq.1).

$$D_{UV} = \int_{t_0}^{t_1} I_{UV}(t)\, dt \tag{1}$$

The UV-velocity v_{UV} (m/s) can be converted into the exposure time t_{UVexp} (s) by taking into account the emission window length L_{UV} (m) of the UV-LED source (see Eq.2).

$$t_{UVexp} = \frac{L_{UV}}{v_{UV}} \tag{2}$$

The following calculation demonstrates the interrelation between exposure time and the UV-velocity 200 mm/s and emission window length 10 mm (see Eq.3).

$$t_{UVexp} = \frac{10mm}{200\ mm/s} = 50\ ms \tag{3}$$

UV-velocity is referring to the speed with which the chuck passes the UV-curing area. Print-velocity defines the speed at which the chuck moves underneath the printhead during the jetting process. This parameter also determines the maximum jetting frequency at which the printhead has to operate for this print job. The actual jetting frequency depends on the pattern, but will always be a fraction of the maximum jetting frequency. The jetting frequency for the two print-velocities 400 mm/s and 200 mm/s are 11.34 kHz and 5.68 kHz, respectively, which is well below the maximum firing frequency limit of 27 kHz posed by the printhead's specifications. Following print parameters remained unchanged for all trials: Print resolution 720.6 dpi, UV-intensity 4 W/cm^2, and general process velocity 400 mm/s. General process velocity refers to the speed of the chuck when moving outside the process area of printing and curing, in other words, when the chuck is not passing a printing printhead or an activated UV-source. Once the chuck passes the "printing process area" or the "curing process area", the velocity parameters "print-velocity" or "curing-velocity" will be applied (see Fig. 3).

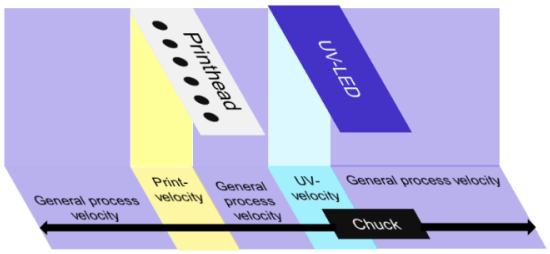

Fig. 3. Different areas along the scanning axis assign different velocities to the chuck

UV-curing took place twice between each swath, one in printing direction, one in the reverse direction. The specimens were printed in a single-pass manner (see Fig. 4). The printing was conducted at a distance between substrate and nozzle plate of 800 µm.

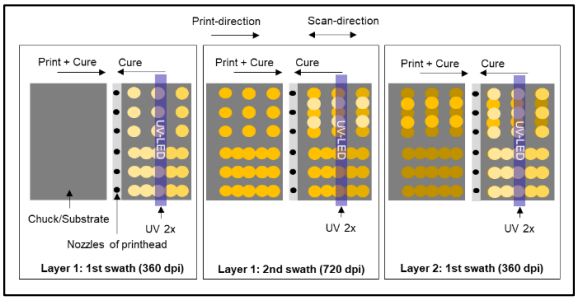

Fig. 4. Print and curing sequences per layer (single-pass printing and bidirectional curing)

Two base layers were printed on the substrate (PET foil, thickness 110 µm) prior to printing the test specimens in order to decouple the obtained results from the substrate properties. Using a base layer based on the same material as the test specimen ensures that the results of this study can be transferred to any other substrates. Without the utilization of base layers, the results would be governed by the condition of the substrate as the wetting behavior of a droplet depends on the liquid/solid interface interaction. The height of the base layer is 48 µm (height per layer is 24 µm). The pre-trials showed, that the following printing parameters for the base layers generated an almost smooth layer: print resolution 720.6 dpi, general process velocity 200 mm/s, print-velocity 200 mm/s, UV-exposure time 50 ms and UV-irradiance 4 W/cm^2. A print resolution of 720.6 dpi, that is a droplet center-to-center distance of 35.25 µm, guarantees an overlap of the deposited droplets. Droplets printed with the next lower print resolution 360.3 dpi were placed too far apart, resulting in insufficient overlapping. Printing only one base layer leads to several void areas (see. Fig. 5, red circle), indicating insufficient amount of material. Two base layers still exhibited few faulty areas, but in much smaller degree, therefore can be considered acceptable. Printing more layers eliminated these imperfections, but the surface becomes uneven/wavy instead. The wavy topology is most likely caused by a surplus of deposited material. In order to minimize the influence of an uneven surface on the droplet spreading behaviour, 2 base layers for all trials were printed to maintain a smooth base.

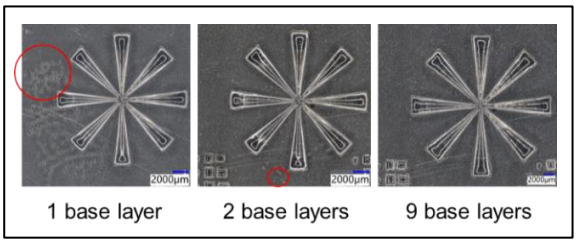

Fig. 5. Surface quality of the base layer with 1, 2 and 9 layers.

In order to assess the resolution limit, several images of the printed specimens were recorded under the optical microscope Keyence VHX-7000. The recorded images were then evaluated according to the three-level assessment scale 0, 0.5 and 1. The value 0 corresponds to the ideal condition which describes non-merged individual lines (see Fig. 6). Partially merged lines are valued as 0.5 which marks the threshold between individual lines and fully merged lines. The grade 1 is reserved for elements which are fully merged. The printing of specimens with the same conditions were repeated triple times and as a result, some specimens with the same printing condition yielded slightly different results. An arithmetic averaging of the results was not applied as the levels 0, 0.5 and 1 deployed in this investigation are to be regarded as a qualitative scale. Instead, all results were treated as followed: Once one of the specimens among a group of identical condition showed partial or full merging (level 0.5 or 1.0), the entire group of these trials will be given the more conservative grade which is either 0.5 or 1.0. This approach was considered more suitable as the onset of merging is an undesirable state in 3D inkjet printing and the aim of the investigation is to define a threshold between merging and no merging. The lines that are printed parallel to print direction (PD) and those printed perpendicular to print direction (PD90°) were assessed separately. The printing condition of each specimens and the printing order are displayed in Table 1.

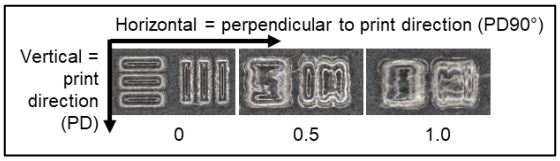

Fig. 6. Assessment scale for evaluating the condition of the printed structure (grade 0= no lines merged, 0.5=partially merged, 1=fully merged)

Table 1
Specimens overview

Specimen No.	General process velocity (mm/s)	Print resolution (dpi)	Print-velocity (mm/s)	UV-exposure time (ms)
1	400	720.6	400	50
2	400	720.6	200	50
3	400	720.6	200	100
4	400	720.6	400	100
5	400	720.6	400	50
6	400	720.6	200	50
7	400	720.6	200	100
8	400	720.6	400	100
9	400	720.6	400	50
10	400	720.6	200	50
11	400	720.6	200	100
12	400	720.6	400	100

3. Results

The data points in the following Figure (Fig. 7) display the element at which partial and full merging of the printed lines occur. Interestingly, for all trials, the lines of element 1 (nominal line spacing 500 µm) remained well-separated (no data point) even though the aspect ratios multiplied. In general, the onset of merging seems to not differ much for different specimen heights, while the line spacing (each element corresponds to a particular distance) or the line width and the printing condition seem to determine the resolution limit.

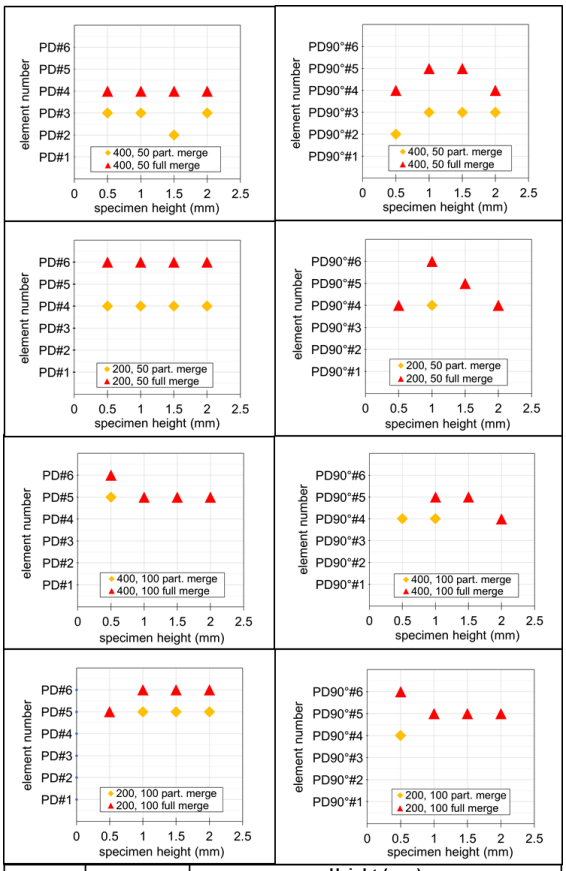

		Height (mm)			
		0.5	1.0	1.5	2.0
Element	Line spacing or width (µm)	Aspect ratio height/width (-)			
1	500	1	2	3	4
2	445.45	1.12	2.24	3.37	4.49
3	396.85	1.26	2.52	3.78	5.04
4	353.55	1.41	2.82	4.24	5.66
5	314.98	1.59	3.17	4.76	6.35
6	280.62	1.78	3.56	5.34	7.13

Fig. 7. The merging elements in print direction (PD) (left column) and perpendicular to print direction (PD90°) (right column) for different printing conditions (print-velocity (mm/s), UV-exposure time (ms))

The next Figure (Fig. 8) shows an excerpt of the results and includes images from the specimens based on which the evaluation has been performed. It is interesting to note, that for all specimens the actual width of the printed lines is much broader than the actual line spacing.

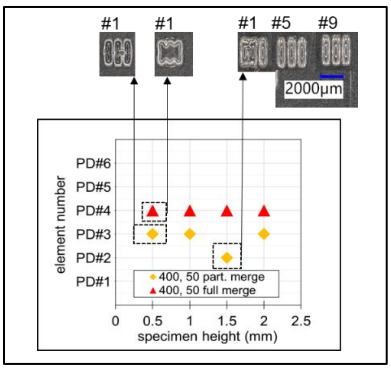

Fig. 8. Results of the trials printed with 400 mm/s print-velocity and 50 ms UV-exposure time. The images in the top show the corresponding specimens (specimen number 1, 5 and 9) based on which the evaluation has been conducted.

Fig. 9 displays the averaged line spacing (nominal values) of the PD- and PD90°-lines at which the merging of the elements has been observed. The curves are almost overlapping, suggesting that the merging is rather governed by the line spacing (or line widths) than by the specimen heights/aspect ratio of the lines (under the same printing condition) as one data point represents the average value of four specimens with varying heights. A large standard deviation would indicate that the line space or line width at which merging takes place vary according to the printed height of the specimen, while 0 means that the merging happens consistently at the same element along all heights. In this investigation, the merging for the print condition 1 (print-velocity 400 mm/s, UV-exposure time 50 ms) for both PD90°- and PD-lines is located at an average value of 409 µm ± 21.04 µm, which means mainly at E3. For the other print conditions the merging happens either at element number E4 or E5. The standard deviations for the PD-lines are 0, and for the PD90°-lines ± 16.70 µm (see Table 2). Overall, the fluctuations stay well below the increments between two subsequent elements and can therefore be regarded as negligible.

Table 2
Averaged line spacing (or line widths) of merging elements (nominal values, n=4)

	Print condition (print-velocity (mm/s), UV-exposure time (ms)	Average line spacing (or line widths) (µm)	Standard deviation (µm)	Percentual deviation (%)
PD-lines	400, 50	409.00	21.04	5.15
	200, 50	353.55	0	
	400, 100	314.98	0	
	200, 100	314.98	0	
PD90°-lines	400, 50	409.00	21.04	5.15
	200, 50	343.91	16.70	4.86
	400, 100	343.91	16.70	4.86
	200, 100	324.62	16.70	5.14

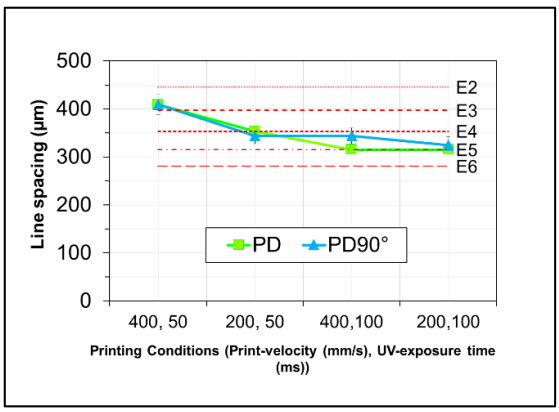

Fig. 9. The averaged nominal line spacing (or line widths) of merging lines in print direction (PD) and perpendicular to print direction (PD90°) (n=4) with the nominal values of the elements E2 to E6 indicated in red

The influence of print parameters on the feature resolution limit can also be concluded from Fig. 9. For both, PD90°- and PD-lines, reducing the print-velocity from 400 mm/s to 200 mm/s (1st and 2nd data points) at 50 ms UV-exposure time shifts the resolution limit to the next smaller feature. For specimens cured with

100 ms UV-exposure time, the same improvement could only be seen for the PD90°-specimens (3rd and 4th data point from left), while the PD-lines merged at the same element. Smaller individual features can also be achieved by increasing the UV-exposure time from 50 ms to 100 ms (2nd/4th and 1st/ 3rd data point from left), regardless of the print-velocity. Overall, the smallest line spacing achieved in this investigation was 353.55 µm.

4. Discussion

The results show that the aspect ratio of the printed specimens does not direct the limit of when two adjacent features can still be printed as individual elements. The applied UV-dose in this investigation most likely was still great enough so that no wet materials ran down the side of the previous deposited layers. No additional influence of the specimen height, at least for the aspect ratios 1 to 7.13 (between a height of 500 µm, 21 layers, and 2000 µm, 87 layers) and a nominal line width between 280.62 µm (element number 6) and 500 µm (element number 1), on the feature resolution limit could be observed. Instead, the spatial periodicity of the printed lines determines whether merging occurs or not. This observation can be explained by the spreading behaviour of a droplet upon impacting the substrate due to the intermolecular interaction between the liquid and solid material [16]. The droplet spreads until it reaches an equilibrium state or until it is solidified by curing, which means that the border of a wet layer is subject to spreading as well until it is fully cured. Depending on the distance between two adjacent features (under the same curing condition), the moving contact line might eventually touch and merge (see Fig. 10).

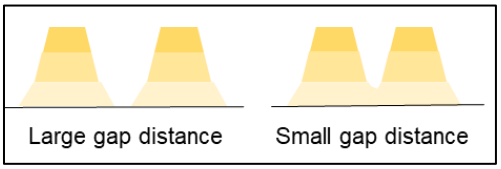

Fig. 10. Schematic illustration of the relation between gap distance and merging.

It has been detected that the results of the PD90°-lines are subject to greater deviations compared to the PD-lines (although still very small), which might indicate a less accurate droplet positioning in printing direction (Fig. 11).

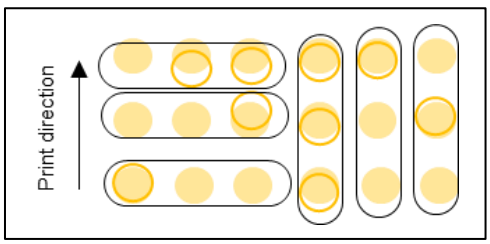

Fig. 11. An illustration on the influence of droplet positioning inaccuracy along the print direction and the merging behavior. The darker circles represent droplets which are outside the expected position

Although the applied print-velocities ensured that the resulting printing frequency stayed below the maximum printing frequency of the printhead, an effect of print-velocity on the feature resolution limit was still visible for some of the printed elements. For both the PD90°- and PD-lines, which were cured with 50 ms UV-exposure time, the resolvable element dropped from 409 µm (mainly element 3) to about 348 µm (mainly element 4) when reducing the print speed. The merging threshold for PD90°-structures decreased from about 348 µm (mainly element 4) to 314 µm (mainly element 5) when transitioning from 400 mm/s to 200 mm/s at 100 ms UV-exposure duration. The threshold of merging for the PD-elements, on the contrary, did not change and remained at 314.98 µm (element 5).

If only the results of the PD90°-structure are to be regarded, following two hypotheses for the influence of print-velocity on the results could be worth considering: First, the chosen print frequencies, even though below the maximum print frequency, still have an effect on the droplet formation. The droplet size or velocity might have reduced considerably at 400 mm/s (print frequency 11.34 kHz) which makes the flying droplet to be more sensitive to aerodynamic drag effect [9] and therefore more prone to positional error. Moreover, a slower chuck-speed may allow a more precise placement of the droplets as it causes less turbulences in the vicinity of the chuck and printhead [9]. Second, a higher print speed reduces the time between droplet impact and curing, therefore stopping the spreading of the droplet contact line at an earlier stage and allowing lines to be printed more closely without merging. If the results of the PD-structure are to be included, the latter hypothesis would not be applicable, since the merging limit did not change when exposing the element to a curing of 100 ms. The positional error, and assuming that the error deviation concerns only the print direction, could explain why the PD-lines did not improve.

The improvement of the achievable feature resolution by increasing the UV-exposure time is due to the increased amount of UV-dose to which the specimen is exposed to. The degree of curing is governed by the amount of UV-dose which is defined as the temporal integral of UV-intensity [15]. An UV-exposure of 100 ms means that the printed droplets are exposed to UV-radiation twice as long as a curing for 50 ms. Furthermore, the beneficial effect of an increased UV-exposure time seems to be enhanced when a print-velocity of 400 mm/s is applied. PD-lines can be printed 94.02 µm closer, meaning that the threshold of merging can be shifted to about 1 to 2 elements. A similar benefit could be observed for PD90°-structures as well. A print-velocity of 200 mm/s allows only a reduction of line space of up to 38.57 µm (PD-lines) and 19.29 µm (PD90°-lines) without leading to merging, which equals to an improvement towards the next element. The difference between the print-velocities might be caused by the size of the printed lines. Most likely, the actual printed lines are slightly larger when printing with 200 mm/s than with 400 mm/s, which also means that the boundary of these lines are located much closer to each other. This enlarging effect could be caused by the increased amount of time that is passing between the impact of droplets onto the substrate and the curing. As mentioned previously, this print-to-curing time defines the amount of spreading and the shape of the droplet until it is cured [13]. A stronger curing, however, can

result in a strong warping of the specimen, which was also present for the specimens cured with 100 ms exposure time.

Inkjet printing produces droplets in the picolitre range, therefore the resulting droplet size on the substrate and the accuracy that comes with it stays within few microns. Nevertheless, the actual achievable final droplet size is governed by the type of printhead (nominal droplet volume), printhead settings (waveform, print frequency), the substrate condition and the print process parameters [10]. In this study, the printhead generated droplets of 28 pL in volume. The droplet sizes on the substrate achieved for this print and curing setting are at least 170 µm in diameter. Considering these conditions, the resolvable feature cannot be smaller than 205.27 µm (droplet size 170 µm plus droplet center-to-center distance 35.27 µm) as a print resolution of 720 dpi requires at least two droplets to be printed in one layer. The smallest resolvable feature of 353.55 µm corresponds to this theoretical consideration, but still exceeds the estimated feature size. This discrepancy can be explained by the fact that the droplet size was determined for one layer of droplets, while in 3D-printing multiple droplet are stacked on top of each other. The layer-wise build-up might have added material in excess which has also been observed for printing more than one base layers. Since the features are rather small in dimension, the excessive material for the line might run down along the sidewall and enlarged the lines. This also could explain, why the obtained lines seemed to be wider than the nominal value as the actual line spacing is narrower than the line width (the test structure is supposed to have line spacings and line widths of the same size). Thus, the concluded value 353.33 µm can be only regarded as a nominal value, but the actual resolvable gap distance might be slightly narrower (and the line width slightly larger). A lower print resolution or halftoning [10] might reduce the amount of material. In this study, the next lower print resolution 360 dpi could not be applied, as the resulting center-to-center distance of the droplet were too far apart to be able to print proper lines with parallel edges.

Nevertheless, the USAF test structure serves as a useful tool to qualitatively assess the influence of print parameters on feature resolution.

5. Conclusions

This investigation showed that the USAF test coupon, originally intended for calibrating optical devices, can be used for 3D inkjet printing as well. Several heights of the USAF test chart group 0 have been printed and qualitatively assessed in terms of the onset of merging with changing printing parameters, namely UV-exposure time and print-velocity. The examined aspect ratios were 1 to 7.13 with the targeted nominal heights 0.5 mm, 1 mm, 1.5 mm and 2 mm and nominal widths ranging from 280.62 µm (element number 6) to 500 µm (element number 1). The thickness of one printed layer was 24 µm. Following observation were concluded from this examination:

- The print parameter settings (print-velocity and UV-exposure time) and the spatial periodicity of the element determines whether two adjacent lines merge or not. The smallest resolvable element achieved in this investigation was 353.55 µm.
- The aspect ratios did not show any influence on the merging behavior.
- Smaller features could be resolved for both PD90°- and PD-lines by doubling the UV-exposure time. The merging, originally taking place at either element 2 (nominal line spacing 445.45 µm) or 3 (nominal line spacing 396.85 µm), could be in this case shifted to the element 4 (nominal line spacing 353.55 µm) or 5 (nominal line spacing 314.98 µm).
- The improvement of feature resolution by lowering the print-velocity was not as significant as when increasing the UV- exposure time and could only be observed for the PD90°-lines.
- The element, for which merging could be determined for the PD90°-lines, is shifting between the neighboring elements much more often than for the PD-lines which suggests that the deposition of the droplets in print-direction is subject to deviations as well.
- The USAF test coupon is deemed useful to study the effect of printing parameters on feature resolution and to assess the influence qualitatively. For quantitative studies, the exact geometrical dimensions of the pattern should be recorded and the ratio between line width and line spacing modified as well.

In order to fully understand the effect of print-velocity on feature resolution, this experiment needs to be extended by systematically investigating the positional accuracy and the droplet formation by means of a drop-watcher. Moreover, further studies should look into the relation between print-to-curing time, the wetting behaviour of the printed layer and the achievable feature resolution while taking warping into consideration. For future studies and quantitative statements, the exact geometrical dimensions of the printed structure and the droplets should be considered. The number of trials and further parameters (e.g. ratio between line widths and line spacing, droplet volume in dependence of the firing frequency, droplet size on substrate and printed layer in dependence of the curing settings) should be included in the experiment as well in order to obtain a comprehensive understanding.

Acknowledgements

This work was carried out with the support of the Karlsruhe Nano Micro Facility (KNMFi, www.knmf.kit.edu) a Helmholtz Research Infrastructure at Karlsruhe Institute of Technology (KIT, www.kit.edu) and under the Helmholtz Research Programme MSE (Materials Systems Engineering) at KIT.

References

[1] M. Fogarasi, K. Snodderly, A. Herman, S. Guha, and D. Porter, "Benchtop assessment of sealing efficacy and breathability of

additively manufactured (AM) face masks," *Addit Manuf,* vol. 67, p. 103468, Apr 5 2023, doi: 10.1016/j.addma.2023.103468.

[2] V. Vashist, N. Banthia, S. Kumar, and P. Agrawal, "A systematic review on materials, design, and manufacturing of swabs," *Annals of 3D Printed Medicine,* vol. 9, 2023, doi: 10.1016/j.stlm.2022.100092.

[3] E. Panettieri, G. Bertolino, and M. Montemurro, "Hands-free printed door opener to limit the spread of Coronavirus: Design through topology optimization," *Composites Part C: Open Access,* vol. 9, 2022, doi: 10.1016/j.jcomc.2022.100316.

[4] A. Salandin, A. Quintana-Gallardo, V. Gómez-Lozano, and I. Guillén-Guillamón, "The First 3D-Printed Building in Spain: A Study on Its Acoustic, Thermal and Environmental Performance," *Sustainability,* vol. 14, no. 20, 2022, doi: 10.3390/su142013204.

[5] J. Parkes. "Joris Laarman's 3D-printed stainless steel bridge finally opens in Amsterdam." dezeen. https://www.dezeen.com/2021/07/19/mx3d-3d-printed-bridge-stainless-steel-amsterdam/ (accessed 2023-05-02.

[6] *ISO/ASTM52900:21 Additive manufacturing — General principles — Fundamentals and vocabulary*, I. I. O. f. Standardization), 2021-11 2021. [Online]. Available: https://www.astm.org/f3177-21.html

[7] Y.-L. Cheng and T.-W. Tseng, "Study on driving waveform design process for multi-nozzle piezoelectric printhead in material-jetting 3D printing," *Rapid Prototyping Journal,* vol. 27, no. 6, pp. 1172–1180, 2021, doi: 10.1108/rpj-05-2019-0120.

[8] A. B. Aqeel, M. Mohasan, P. Lv, Y. Yang, and H. Duan, "Effects of the actuation waveform on the drop size reduction in drop-on-demand inkjet printing," *Acta Mechanica Sinica,* vol. 36, no. 5, pp. 983–989, 2020, doi: 10.1007/s10409-020-00991-y.

[9] C. Rodriguez-Rivero, J. R. Castrejón-Pita, and I. M. Hutchings, "Aerodynamic Effects in Industrial Inkjet Printing," *Journal of Imaging Science and Technology,* vol. 59, no. 4, pp. 40401-1-40401-10, 2015, doi: 10.2352/J.ImagingSci.Technol.2015.59.4.040401.

[10] A. Elkaseer, S. Schneider, Y. Deng, and S. G. Scholz, "Effect of Process Parameters on the Performance of Drop-On-Demand 3D Inkjet Printing: Geometrical-Based Modeling and Experimental Validation," (in eng), *Polymers,* vol. 14, no. 13, 2022, doi: 10.3390/polym14132557.

[11] X. Jia, B. Huang, W. X, and M. Sun, "Study on the influence of printing conditions on the curing of UV ink," in *NIP27: 27th International Conference on Digital Printing Technologies*, S. Society for Imaging and Technology Eds. Springfield, Va.: IS & T Society for Imaging Science and Technology, 2011, pp. 399–401.

[12] P. Zhao *et al.*, "Modelling the influence of UV curing strategies for optimisation of inkjet based 3D printing," *Materials & Design,* vol. 208, p. 109889, 2021, doi: 10.1016/j.matdes.2021.109889.

[13] W. Zhou, D. Loney, A. G. Fedorov, F. L. Degertekin, and D. W. Rosen, "Shape evolution of multiple interacting droplets in inkjet deposition," *Rapid Prototyping Journal,* vol. 21, no. 4, pp. 373–385, 2015, doi: 10.1108/rpj-12-2013-0131.

[14] A. Elkaseer, K. J. Chen, J. C. Janhsen, O. Refle, V. Hagenmeyer, and S. G. Scholz, "Material jetting for advanced applications: A state-of-the-art review, gaps and future directions," *Additive Manufacturing,* vol. 60, p. 103270, 2022, doi: 10.1016/j.addma.2022.103270.

[15] P. F. Jacobs, "Fundamentals of Stereolithography," in *Proceedings for the 1992 International Solid Freeform Fabrication Symposium*, A. The University of Texas at Ed., 1992.

[16] Z. Wang, D. Orejon, Y. Takata, and K. Sefiane, "Wetting and evaporation of multicomponent droplets," *Physics Reports,* vol. 960, pp. 1-37, 2022, doi: 10.1016/j.physrep.2022.02.005.